JOURNAL OF AIRCRAFT
Vol. 37, No. 6, November–December 2000

Lift Augmentation on Delta Wing with Leading-Edge Fences and Gurney Flap

Mark D. Buchholz*
Lockheed Martin Aeronautics Company, Palmdale, California 93599
and
Jin Tso†
California Polytechnic State University, San Luis Obispo, California 93407

A wind-tunnel experiment was conducted on a 60-deg delta wing at low speeds and low angles of attack to determine the lift augmentation effects of the leading-edge fences and a Gurney flap. Lift, drag, pitching moment, and surface pressures were measured, accompanied by vapor and oil-film flow visualizations. Both the leading-edge fences and the Gurney flap increase lift. They are shown to shift the lift curve by as much as 5 and 10 deg, respectively. The fences aid in trapping vortices on the upper surface, thereby increasing suction. The Gurney flap, on the other hand, improves circulation at the trailing edge. The lift augmentation effects of these two devices are roughly additive, resulting in high lift gain.

Nomenclature

C_D = drag coefficient, $D/q_\infty S$
C_L = lift coefficient, $L/q_\infty S$
C_M = pitching moment coefficient, $M/q_\infty S c_r$, about 25% mean aerodynamic chord
C_p = pressure coefficient, $(p - p_\infty)/q_\infty$
c = local airfoil chord
c_r = wing root chord
D = drag force
h = fence height; flap chord
L = lift force
M = pitching moment
p = surface static pressure
p_∞ = freestream static pressure
q_∞ = freestream dynamic pressure, $\rho U_\infty^2/2$
Re = Reynolds number, $\rho U_\infty c_r/\mu$
S = reference area, wing area plus projected device area
t = wing thickness
U_∞ = freestream velocity
x = chordwise coordinate
y = spanwise coordinate
α = angle of attack
Δ = gain in force coefficient from device (i.e., ΔC_L, ΔC_D)
Λ = sweep angle
μ = absolute viscosity
ρ = density
ϕ = fence angle

Introduction

DELTA wings of low aspect ratio have long been used for supersonic aircraft because of their favorable wave drag characteristics. The delta wing generates large vortex lift at high angles of attack, which allows for its flight at low-speed conditions. The vortex lift is due to the leading-edge separation that results in roll up of vortices above the wing. The vortices, in turn, create high-suction regions near the leading edge, as well as maintaining attached flow inboard.

Received 29 November 1999; revision received 24 July 2000; accepted for publication 25 July 2000.

*Research Specialist, Aerodynamics Department, 1011 Lockheed Way.
†Professor, Aerospace Engineering Department.

A variation of the delta wing was considered for the High-Speed Civil Transport (HSCT). To reduce noise and to avoid tail strike or impairment of the pilots' view, the HSCT needs to fly at low angles of attack during takeoff and landing. This, however, requires significant lift augmentation on the delta wing. Among various passive and active means that could be used to achieve this purpose, the leading-edge fences and the Gurney flap were considered promising enough for initial exploration.

Background

Vortex Trapping with Leading-Edge Fences

Using conformal mapping solutions, Rossow[1] showed in the late 1970s that a vortex could be trapped above an infinite wing with a fence positioned near the leading edge with cross-stream suction applied. The trapped vortex would add apparent thickness and camber to the wing, thereby increasing lift. He later suggested that a rear fence could be employed to aid in trapping the vortex and reduce the required cross-stream suction.[2] Both experimental and numerical results appeared to support these vortex trapping concepts.[3–5] Rossow[2] further speculated on their application to delta wings, where the freestream velocity component parallel to the leading edge would provide the necessary cross-stream suction.

In fact, in a seemingly unrelated experiment on the leading-edge vortex flap (LEVF), Marchman[6] has shown that the constant-chord LEVFs, inverted 40 deg upward (140 deg from the wing upper surface) on a 60-deg delta wing, can increase the lift coefficient by about 0.18 at angles of attack up to where the stall occurs. Similar effects were seen for tapered LEVFs inverted 30 deg upward on a 75-deg delta wing. Such inverted LEVFs, as he speculated, could be useful in landing. Lift increases by vortices trapped behind tapered and constant-chord leading-edge fences (flaps normal to wing surface) were later reported by Buchholz and Tso[7,8] for a 60-deg delta wing at low angles of attack, although no similar increases were observed for the two-fence configurations tested. For the constant-chord fences, in particular, they observed that only those with an opening in the apex region produce noticeable lift increases. This is consistent with the recent observation by Traub and Galls[9] that neither upper nor lower (full-span) constant-chord leading-edge Gurney flaps on a 70-deg delta wing produce any noticeable lift increases at angles of attack up to the stall angle. In a separate water-channel experiment on a 70-deg sweep delta wing at angles of attack from 16 to 35 deg, Deng and Gursul[10] have shown the vortices trapped by LEVFs deflected 60–150 deg from the wing upper surface. They concluded that the breakdown of the trapped vortices depends strongly on the flap deflection angle and the angle of attack.

Gurney Flap

The Gurney flap was originally used at the trailing edge of a rectangular race-car wing. It was a flat plate deflected 90 deg, perpendicular to the airfoil chord line. Numerous wind-tunnel tests on the Gurney flap have been done on both single- and multielement airfoils and some on straight and tapered wings.[11,12] The flap chord was typically 1–5% of the airfoil chord. According to Liebeck,[13] race-car testing by Gurney demonstrated improved downforce with the flap. Drag was typically increased for the larger flap chords, but a reduction in drag was noticed for flap chords below 2%. Liebeck hypothesized that with the addition of the flap, separation of the upper surface flow was delayed, allowing for a wake of similar, even lower, momentum deficit than that of the bare airfoil. Water-tunnel visualizations[14] and two-dimensional numerical solutions[15] have supported Liebeck's[13] hypothesis. Experiments with a 5% Gurney flap on a two-element airfoil have also been conducted.[16] Higher lift and lower lift-to-drag ratio L/D were recorded, which is consistent with Liebeck's[13] findings for larger flap chords. The Gurney flap has also been used on an airfoil with vortex generators in concert to generate greater lift enhancement.[17]

The preceding studies were all for airfoils and straight or tapered wings. The Gurney flap, however, could be used at the trailing edge of a delta wing to increase circulation, thereby increasing lift.[7–9] Located at the trailing edge, the Gurney flap also has the advantage of complementing the lift augmentation obtained by the vortices trapped upstream behind the leading-edge fences. Together, these two devices could work in concert to provide a high lift configuration useful to the HSCT during takeoff and landing. With this idea in mind, a wind-tunnel experiment was set out to determine the separate and joint performances of these two devices for a 60-deg delta wing at low speeds and low angles of attack.

Experimental Apparatus and Procedure

Wind Tunnel and Test Models

The experiment was conducted in the 3 ×4 ft (91.4 ×121.9 cm) low-speed wind tunnel in the Aerodynamics Laboratory at California Polytechnic State University, San Luis Obispo, California. Figure 1 shows the schematic of the general flat-plate delta wing model with a 60-deg sweep angle and the three test configurations for the leading-edge fences and the Gurney flap. The delta wing models were all made of clear acrylic. Their leading edges were beveled downward at 45 deg, and the trailing edges were left blunt for flap attachment. The leading-edge fences and the Gurney flaps were also made of acrylic, with sharpened edges. There were all mounted normal to the wing surface, with the fences along the leading edges and the Gurney flaps along the trailing edge.

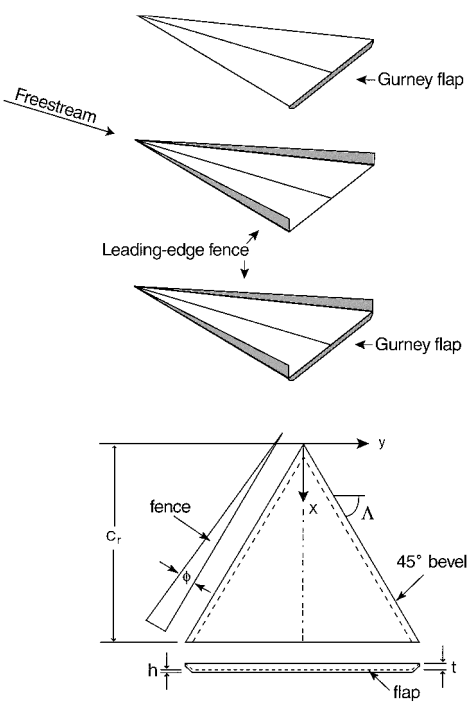

Fig. 1 General schematic of wing model with tapered leading-edge fences and constant-height Gurney flap.

Delta wing models of different sizes were used. The first model had a 25-in. (63.50-cm) root chord and $\frac{3}{4}$-in. (1.91-cm) thickness; it was used for force and moment measurements and for flow visualization with vapor. The second model had a 17.31-in. (43.97-cm) root chord and $\frac{1}{2}$-in. (1.27-cm) thickness and was used for surface flow visualization with oil film. Both models had $\frac{1}{8}$-in.-(0.32-cm-) thick acrylic fences and flaps. The third model had a 24-in. (60.96-cm) root chord and 0.87-in. (2.18-cm) thickness; it was built for surface pressure measurements. The Gurney flap used on this model was $\frac{1}{4}$ in. (0.64 cm) thick, and the tapered leading-edge fences had an included angle ϕ of 5 deg and were $\frac{1}{4}$ in. (0.64 cm) thick. Nine rows of 0.01-in.- (0.025-cm-) diam static-pressure ports were located at 10% root chord intervals on this model. The aft rows contained 20 ports on the wing semispan and 7 ports on each side of the fence; the resolution decreased near the apex region. Inside the wing, clear flexible PVC tubing connected each port to a pressure tap on the trailing edge.

Force and Moment Measurements

A custom-made Aerolab six-component sting balance was used to measure lift, drag, and pitching moment. The wing models were strut mounted with an aerodynamically smooth 0.13-in. (3.3-mm) steel plate on the sting balance, which in turn was connected to an angle-of-attack controller and indicator. The balance's strain gauge outputs were sent through a Hewlett–Packard 3421A data acquisition control unit to a Hewlett–Packard 150 personal computer, where 30 readings over 10-s periods were averaged to obtain the force and moment data. The pitching moment was taken about the 25% mean aerodynamic chord. The force and moment coefficients were calculated based on the wing area plus any projected device area. The gains in force coefficients, that is, ΔC_L and ΔC_D, were calculated by subtracting the coefficient of the bare delta wing from the coefficient of the delta wing with fences or flap. The force and moment measurements were done at the Reynolds number of 8.6×10^5 based on the root chord. For the majority of measurements, the uncertainties are at most ± 0.01 for the lift and drag coefficients and less than ± 0.005 for the pitching moment coefficient. In addition, the accuracy for the angle of attack is within ± 0.1 deg.

Because of the wing thickness, the 45-deg bevel of the leading edges, and the blunt trailing edge, the base delta wing model had a higher lift curve slope than thin delta wings with small bevels on all edges.[18,19] However, because the primary goal of the present experiment was to examine the lift and drag increments of the leading-edge fences and the Gurney flap, no further refinements were made on the models. Also, no wall or blockage corrections were made in calculating the coefficients.

Flow Visualization

Both vapor and oil film were used to visualize flow patterns of the trapped vortices. The vapor was generated by superheating a Rosco fogging fluid flowing through an electrically heated $\frac{1}{32}$-in. (0.79-mm) i.d. steel tube. The outlet of the steel tube was positioned near the apex of the delta wing to allow entrainment of vapor into the vortex core. Surface flow patterns, on the other hand, were visualized using the oil-film technique. In this approach, a mixture of black powdered tempera paint and mineral oil was applied evenly to the white model surface. The wind tunnel was brought quickly up to the test speed and ran until the coating of oil became too thin to flow. Afterward, the surface flow patterns were recorded with a 35-mm camera.

Pressure Measurements

Surface pressures induced by the trapped vortices were measured using a 48-port Scanivalve® (Model 48J9 2373) with a single

pressure transducer rated for a maximum of 0.5 psi differential (3447 Pa) and an accuracy of ±0.06% full scale. The transducer output was sampled via an RC Electronics ISC-16 data acquisition system to an Everex 386 personal computer. Time averages of 256 readings over 2-s periods were taken, and each row of pressure ports was scanned at several angles of attack.

Results and Discussion

Leading-Edge Fences

Figure 2 shows the plots of lift coefficient vs angle of attack for fences with the fence angle ϕ varied from 2 to 8 deg. As seen in Fig. 2, the lift curve for the $\phi = 2$ deg fences still exhibits a quasi-linear behavior with angle of attack, similar to the bare delta wing. With increasing fence height, the delta wing produces greater lift, and the lift increases amount to shifts of the lift curve by about 2–5 deg. The lift curves for the higher fences, however, have an anomaly near $\alpha = 5$ deg. It appears as a short plateau for $\phi = 5$ deg and becomes a pronounced dip for $\phi = 8$ deg. In addition, the slopes of these curves decrease at angles of attack beyond the anomaly. The anomaly is magnified by the plots of the lift gain coefficient in Fig. 3. In general, the lift gain increases with angle of attack below $\alpha \approx 5$ deg and then decreases. This is consistent with the slope change of the lift curve around the anomaly in Fig. 2. It was also noticed that at any angle of attack before the anomaly the lift gain is roughly linearly proportional to the fence angle.

Figures 4 and 5 show the results of C_D and ΔC_D, respectively. As seen in Fig. 4, the higher fences produce higher drag. The anomaly is apparent at $\alpha \approx 5$ deg in the drag coefficient curve for the highest fences. However, unlike its counterpart in the ΔC_L curves, the anomaly is less distinct in the ΔC_D curves in Fig. 5. The drag gain increases until $\alpha \approx 5$ deg but remains nearly constant beyond the anomaly.

A comparison of the plots of L/D vs lift coefficient is shown in Fig. 6. The bare delta wing is seen to have the highest L/D, with a peak of 5.2 at $C_L \approx 0.3$. The peak ratio decreases and becomes less distinct with increasing fence angle. Figure 7 shows the plots of pitching moment vs angle of attack. Despite the anomaly at $\alpha \approx 5$ deg, the overall trend of the moment coefficient is not changed appreciably with the addition of fences.

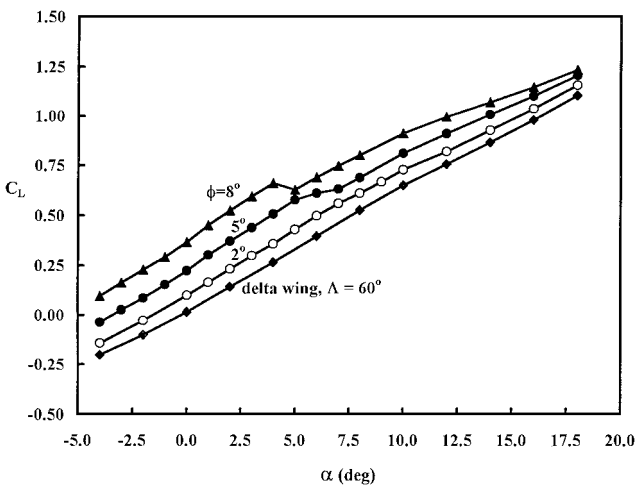

Fig. 2 Effect of fence angle on lift, $Re = 8.6 \times 10^5$.

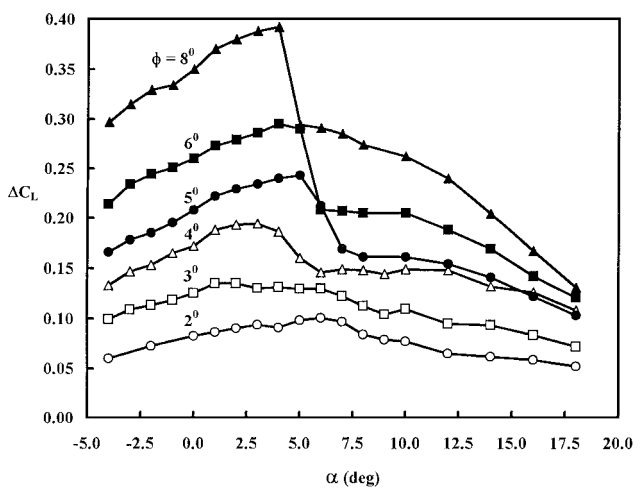

Fig. 3 Effect of fence angle on lift gain, $Re = 8.6 \times 10^5$.

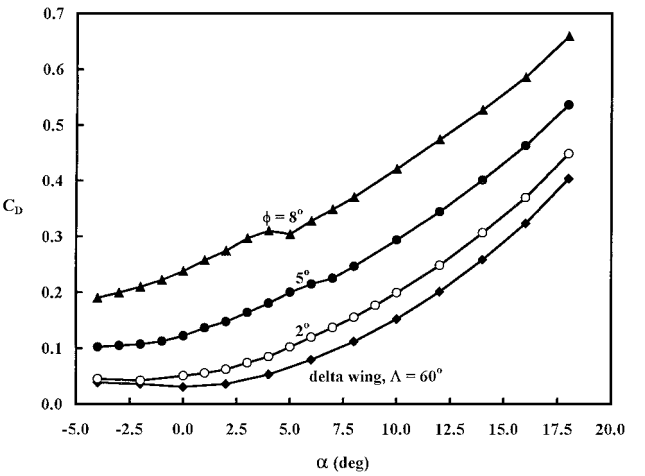

Fig. 4 Effect of fence angle on drag, $Re = 8.6 \times 10^5$.

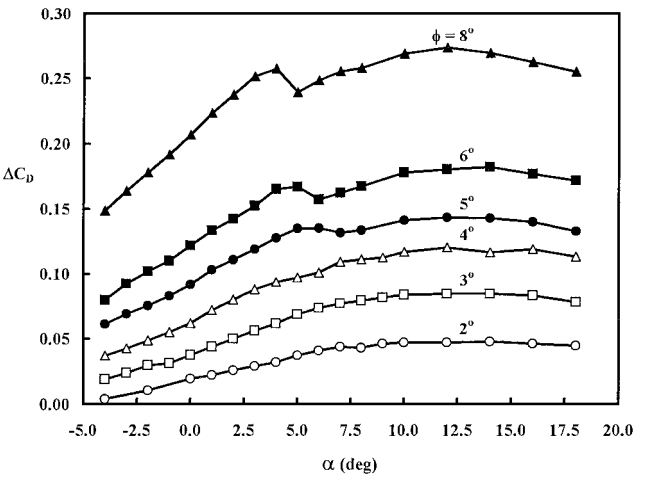

Fig. 5 Effect of fence angle on drag gain, $Re = 8.6 \times 10^5$.

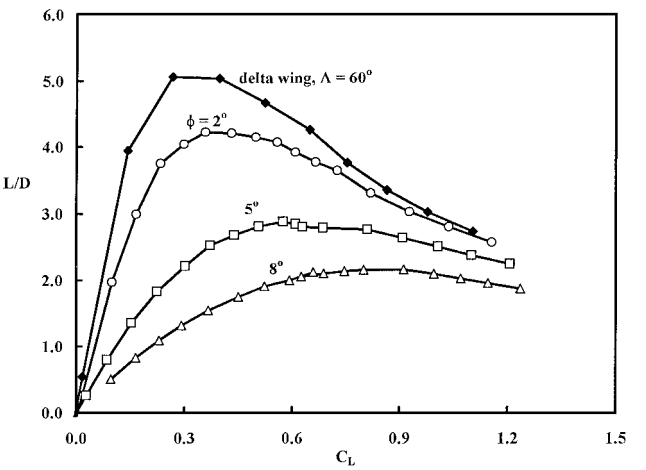

Fig. 6 Effect of fence angle on L/D, $Re = 8.6 \times 10^5$.

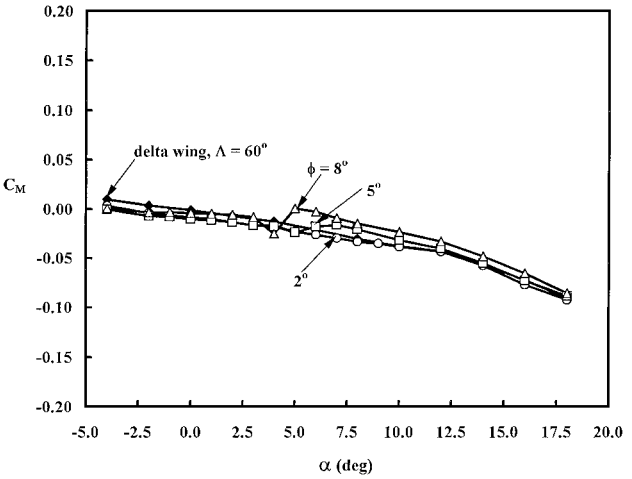

Fig. 7 Effect of fence angle on pitching moment, $Re = 8.6 \times 10^5$.

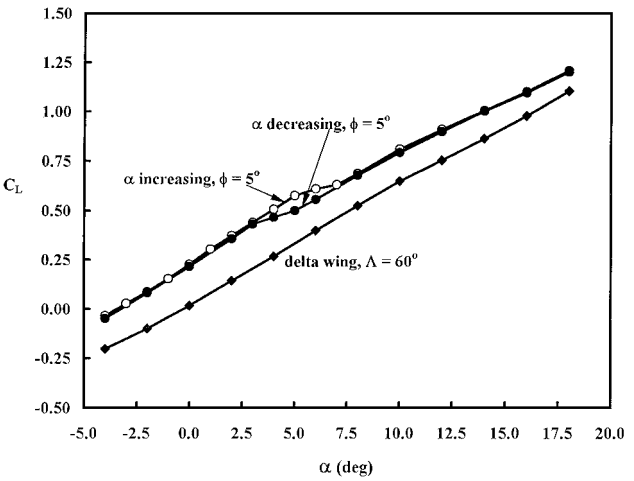

Fig. 8 Hysteresis of the lift coefficient, $Re = 8.6 \times 10^5$.

The results presented in Figs. 2–7 were all measured with increasing angles of attack. With decreasing angles of attack, however, lower lift gains were obtained near the anomaly. Figure 8 shows this hysteresis effect in the C_L vs α plots for the $\phi = 5$ deg fence at $Re = 8.6 \times 10^5$. As seen in Fig. 8, the hysteresis loop exists between $\alpha = 3$ and 7 deg. The upper portion of the loop is from data measured through increasing angle of attack and the lower portion through decreasing angle of attack. On entering the loop from either side of the anomaly region, the lift curve slope is preserved. This suggests that the flow characteristics for $\alpha < 3$ deg are different from those at $\alpha > 7$ deg.

Flow Visualization

To understand better the measured lift increases, both vapor and oil film were used to visualize the flow over the wing. For the bare delta wing at increasing angles of attack, the fogging fluid vapor revealed little evidence of leading-edge vortices at $\alpha = 0$ deg (Fig. 9a). A weak vortex core can be seen at $\alpha = 6$ deg (Fig. 9b), and vortex bursting starts to occur at $\alpha = 14$ deg over the aft portion of the wing. These observations are consistent with previous investigations.[18–20] However, with the addition of the $\phi = 5$ deg fences, the vortex core is distinct at $\alpha = 0$ deg, as shown in Fig. 10a. The case for $\alpha = 6$ deg is similar (Fig. 10b), except that bursting of the vortex core could be seen intermittently above the wing. The bursting point would remain approximately one-third of the root chord behind the trailing edge for 30–60 s, then move up to the trailing edge and back again. This intermittent behavior is captured in Fig. 10c. As the angle of attack is further increased to $\alpha = 10$ deg, the bursting point moves above the wing and stays at a steady location, as shown in Fig. 10d. As the angle of attack decreases, however, the vortex bursting point

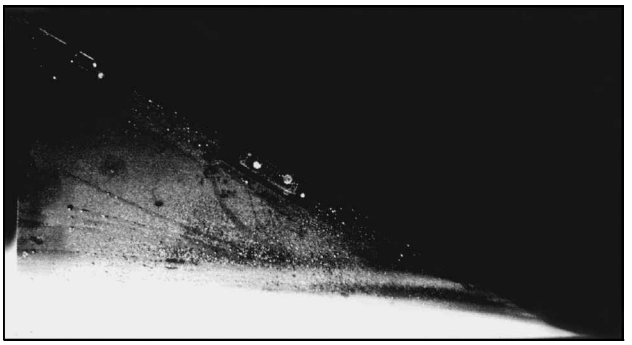

a) $\alpha = 0$ deg

b) $\alpha = 6$ deg

Fig. 9 Vapor patterns on 60-deg delta wing, $Re = 4.3 \times 10^5$.

would move gradually downstream and finally behind the trailing edge at $\alpha \approx 4$ deg. This is consistent with the hysteresis of the lift coefficient reported earlier.

Figure 11 shows the surface oil film patterns for the $\phi = 5$ deg fenced wing. Consistent with the vapor patterns, Fig. 11a shows that the primary vortex is well developed at $\alpha = 0$ deg, and the secondary vortex is seen adjacent to the fence. In between these two vortices is a region showing a braided tertiary pattern. As the angle of attack increases to $\alpha = 10$ deg, Fig. 11b shows that the primary vortex pattern expands at the aft portion of the wing due to vortex bursting. The bursting also smears the region between the primary and secondary vortices. When compared to the water-channel results of Deng and Gursul[10] on a 70-deg delta wing, the breakdown of the vortices trapped by leading-edge fences appears to occur at a lower angle of attack. Their result would suggest that for delta wings of larger sweep angles, higher leading-edge fences could be used for lift augmentation at low angles of attack.

The flow visualization results are consistent with the force and moment measurements reported earlier. The increases in lift and drag coefficient at low angles of attack could easily be explained by the vortices trapped by the fences and the deteriorated lift gains beyond $\alpha \approx 5$ deg by vortex bursting near the trailing edge. The vortex bursting explains the anomalies observed in the lift and drag curves in Figs. 2–7. The explanation is also consistent with previous studies on vortex bursting,[18] which show a drop in lift curve slope when the vortex bursting location moves upstream from the trailing edge.

Although the flow visualizations were observed at $Re = 4.3 \times 10^5$ and 6×10^5, they provided adequate explanations for the lift and drag coefficient trends at $Re = 8.6 \times 10^5$. This relative insensitivity to Reynolds number is likely because the leading-edge vortices are formed by roll up of the shear layers separated at fixed locations, the sharp edges, of the fences. Such weak dependence on Reynolds number is also consistent with the observation by Deng and Gursul[10] that the formation and breakdown of the trapped vortices depend strongly on the leading-edge flap deflection angle and the angle of attack.

Surface Pressure Distributions

Figure 12 shows the surface pressures measured over one-half of the upper surface of the 60-deg delta wing and on both sides of the $\phi = 5$ deg fence. The pressures on the bare delta wing and the

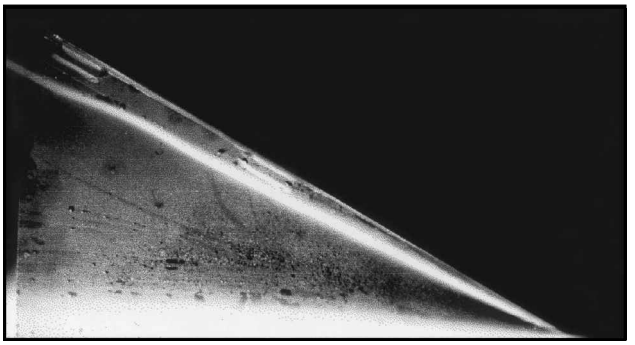

a) α = 0 deg

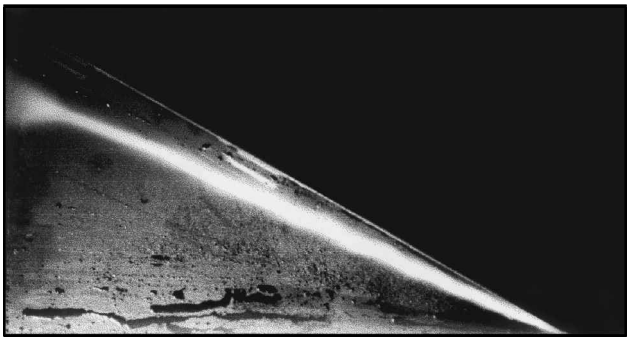

c) α = 6 deg occasionally

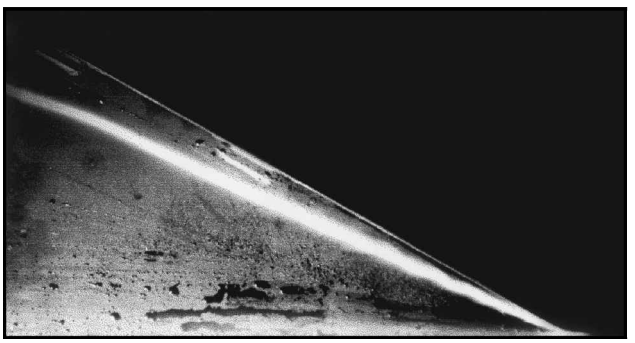

b) α = 6 deg

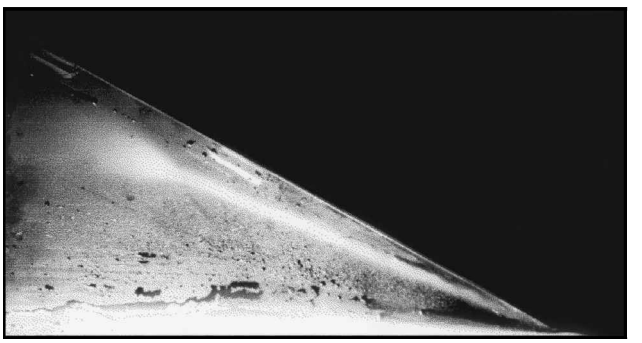

d) α = 10 deg

Fig. 10 Vapor patterns on 60-deg delta wing with ϕ = 5 deg fences, $Re = 4.3 \times 10^5$.

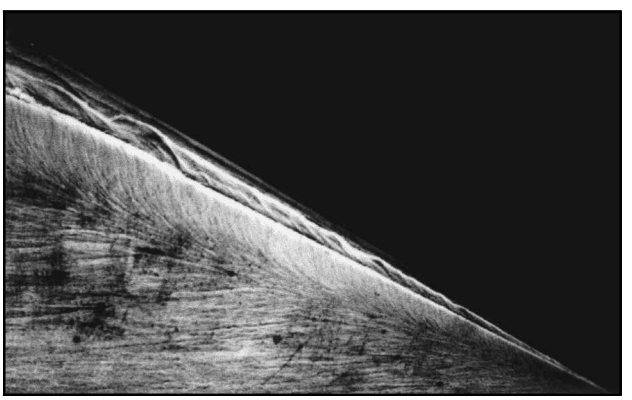

a) α = 0 deg

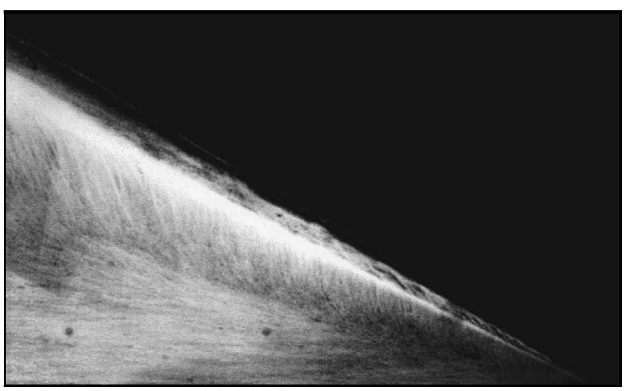

b) α = 10 deg

Fig. 11 Oil patterns on 60-deg delta wing with ϕ = 5 deg fences, $Re = 6 \times 10^5$.

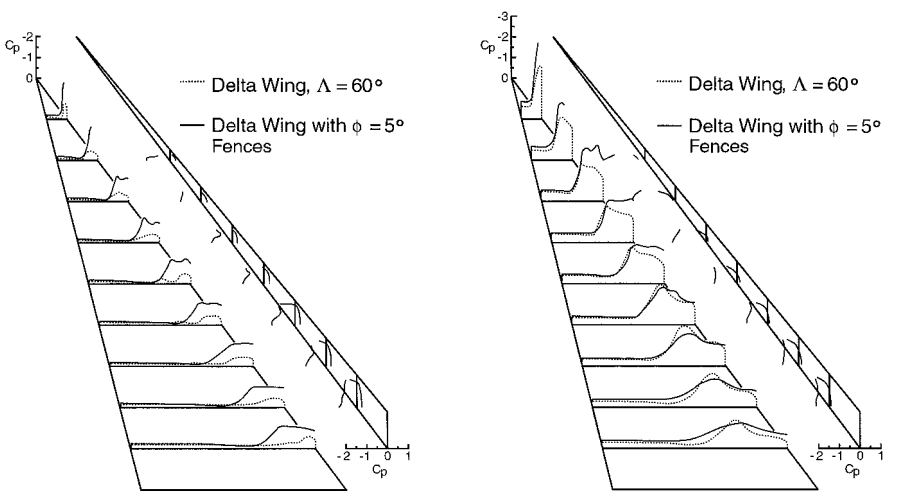

a) α = 0 deg

b) α = 10 deg

Fig. 12 Surface pressure distributions, $Re = 7.9 \times 10^5$.

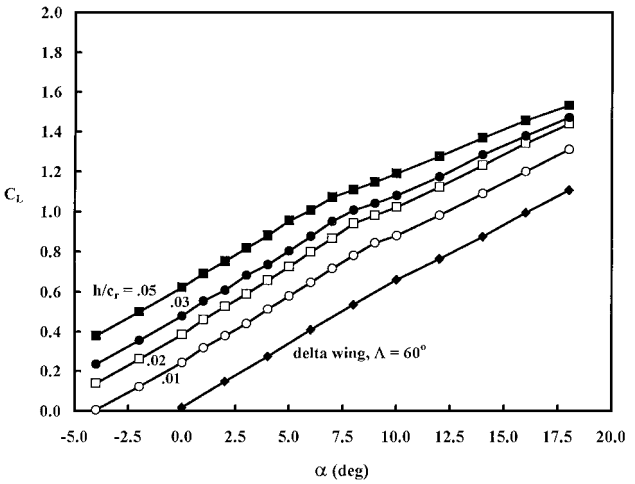

Fig. 13 Lift for constant-height Gurney flap, $Re = 8.6 \times 10^5$.

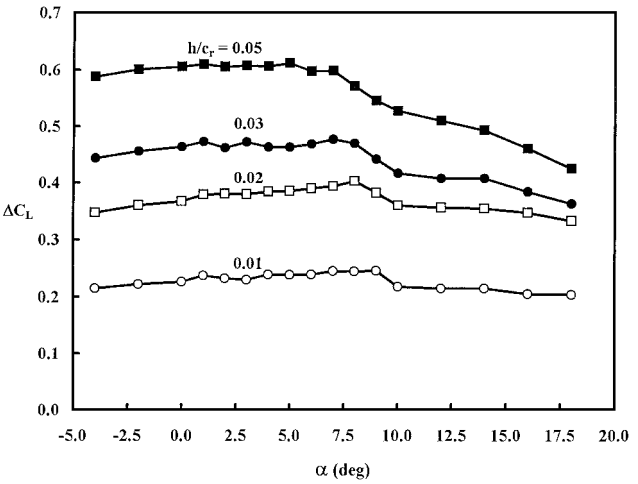

Fig. 14 Lift gain for constant-height Gurney flap, $Re = 8.6 \times 10^5$.

fenced delta wing are compared at $\alpha = 0$ and 10 deg. Generally, the suction on the bare delta wing increases with angle of attack. It is highest near the apex and gradually decreases toward the trailing edge. The buildup of the strong leading edge vortices can be seen as the angle of attack increases from 0 to 10 deg. The high suction peaks near the leading edge are associated with the primary and secondary vortices. The inboard region has substantially less suction than the region under the vortices. Between these regions exists a dip in suction that can be attributed to the reattachment of the primary separation.

The addition of fences creates strong primary and secondary vortices, which impose clear suction peaks on the wing and fence surfaces. In comparison to the bare delta wing, large increases in suction are present at $\alpha = 0$ deg, where the bare delta wing vortex has not yet formed. This is shown in Fig. 12a. At $\alpha = 10$ deg, Fig. 12b shows that the fences still provide a large increase in suction on the forward portion of the wing. However, there is a loss of suction on the aft portion of the wing due to vortex bursting. In both cases, there is a large pressure difference across the fence, which is primarily responsible for the drag increase.

Gurney Flap

In addition to the leading-edge fences, the Gurney flap was attached along the trailing edge of the delta wing to examine its lift augmentation effect. In previous experiments, the Gurney flap was typically tested with airfoils, and its height was a percentage of the local airfoil chord. However, as found in this experiment, an $h/c = 0.05$ tapered flap and an $h/c_r = 0.02$ constant-chord flap had nearly the same lift and drag characteristics. Because of its greater simplicity, smaller area, and smaller maximum height, the constant-chord Gurney flap was used for further testing.

Figure 13 shows the plots of C_L vs α for constant-chord Gurney flaps. As seen in Fig. 13, the lift coefficient increases with increasing flap chord, and the increases amount from 4- to 10-deg shifts of the lift curves. For larger flaps, a decrease in the lift curve slope is seen at angles of attack around $\alpha = 10$ deg. This change is magnified by the lift gain plots in Fig. 14, and it is attributed to vortex bursting. The slope decrease, however, was not expected initially at this angle of attack (compared to 14 deg for the bare delta wing) because the rectangular wing results for the 2% chord Gurney flap would suggest that the flap should decrease the adverse pressure gradient near the trailing edge. Previous studies on vortex bursting have indicated that both high swirl angle and adverse pressure gradient can cause vortex breakdown.[21,22] Because the Gurney flap produces a higher pressure on the lower wing surface, it could cause more flow to circulate around the leading edges, thereby increasing the vortex swirl angle. Consequently, the Gurney flaps used could lead to vortex breakdown at lower angles of attack.

Figures 15 and 16 show the plots of drag and drag gain coefficients. Not surprisingly, the drag coefficient increases with increasing flap chord. L/D is plotted vs lift coefficient in Fig. 17. For higher lift coefficients, similar to the observation by Traub and Galls,[9] the flapped configurations exceed the bare delta wing in efficiency. This advantage, however, is tainted by the flap's high negative pitching moment, as shown in Fig. 18.

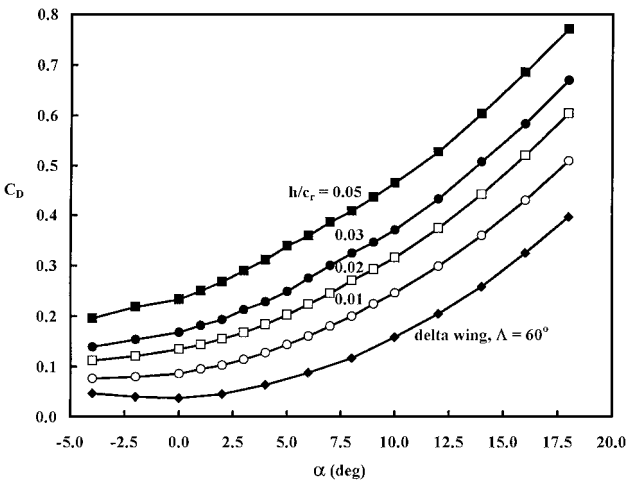

Fig. 15 Drag for constant-height Gurney flap, $Re = 8.6 \times 10^5$.

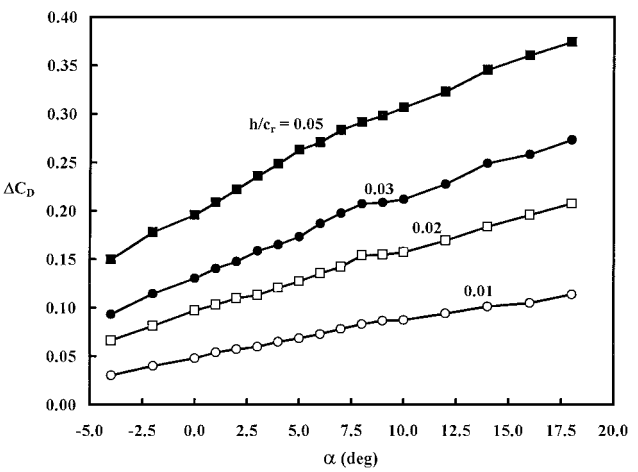

Fig. 16 Drag gain for constant-height Gurney flap, $Re = 8.6 \times 10^5$.

Comparison of Fences and Flaps

The results thus far have shown that both the tapered leading-edge fences and the constant-chord Gurney flap increase the lift of

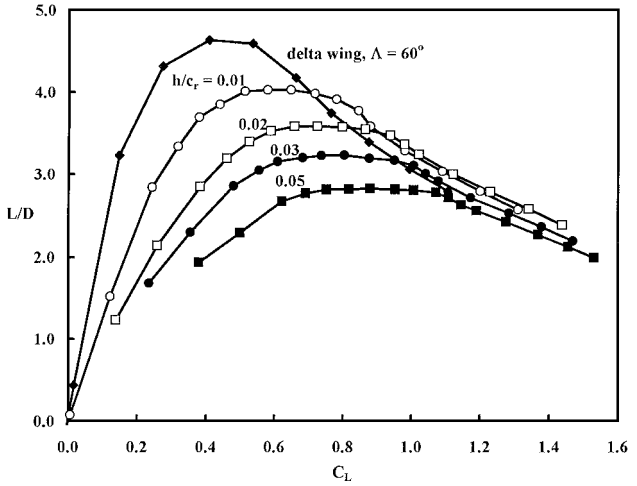

Fig. 17 *L/D* **for constant-height Gurney flap,** $Re = 8.6 \times 10^5$.

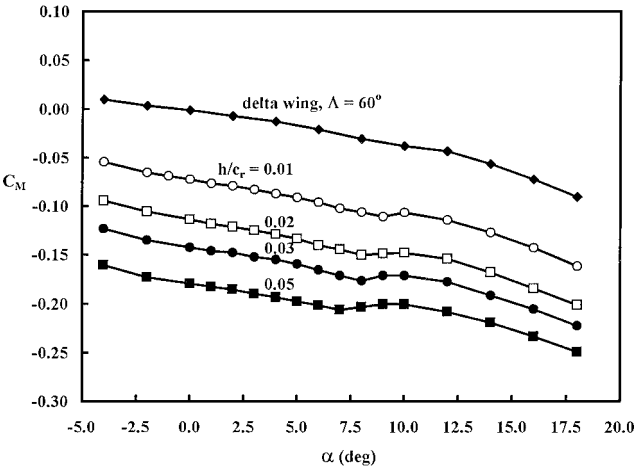

Fig. 18 Pitching moment for constant-height Gurney flap, $Re = 8.6 \times 10^5$.

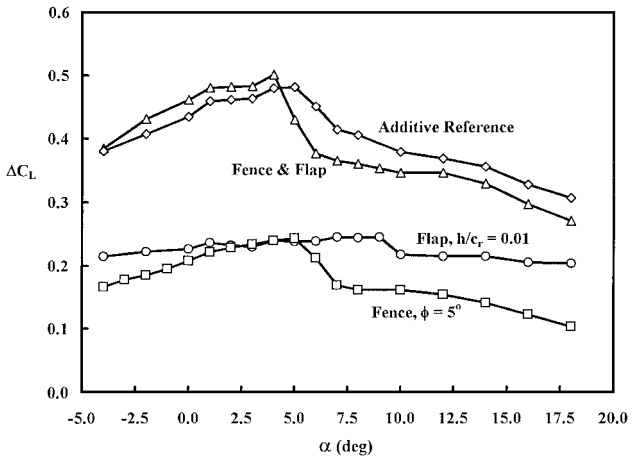

Fig. 19 Gain in lift for combined fence-flap configuration, $Re = 8.6 \times 10^5$.

the 60-deg delta wing at low speeds and low angles of attack. The flap has shown higher L/D efficiency. Compared to the bare delta wing, the fences reduce the L/D, but the Gurney flap increases the ratio at high lift coefficients. Both devices lower the angle of attack at which vortex bursting reaches the trailing edge; the fences fare worse in this aspect. However, the fences produce little change in the pitching moment, superior to the flap's significant nose-down moment.

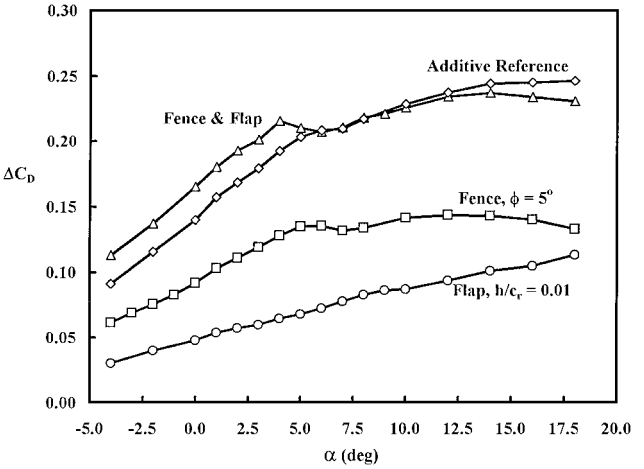

Fig. 20 Gain in drag for combined fence-flap configuration, $Re = 8.6 \times 10^5$.

Despite their differences, the lift augmentation effects of these two devices are almost additive. Figures 19 and 20 show the lift and drag gains of the combined configuration of the $\phi = 5$ deg fences and the $h = 0.01c_r$ flap. The gains of the combined configuration are seen to be fairly close to the sum of the gains of the individual devices. In fact, the combined lift gain before vortex bursting is almost twice the individual gains. This occurs because the primary effect of the leading-edge fences is to increase vortex lift whereas that of the Gurney flap is to improve the circulation surrounding the trailing edge.

Conclusions

A wind-tunnel experiment has been conducted on a 60-deg delta wing with tapered leading-edge fences and a Gurney flap to determine their lift augmentation effects for low-speed and low-angle-of-attack applications during the approach and landing phases of flight. Through different mechanisms, both devices produced large lift augmentations at low angles of attack. The fences aid in trapping vortices to increase suction on the upper surface, whereas the Gurney flap improves circulation at the trailing edge. Shifts in the lift curve by as much as 5 and 10 deg (0.4 and 0.6 increases in lift coefficient) were achieved by the fences and flap, respectively. In particular, the study shows that the individual lift augmentation effects of both devices are roughly additive, creating high lift gain.

Each device, however, has its own disadvantages. The Gurney flap significantly increases nose-down pitching moment. The fences, on the other hand, reduce L/D more when compared to a Gurney flap of about the same maximum lift gain. The higher fences, in particular, precipitate vortex bursting at $\alpha \approx 5$ deg and perhaps should only be used with delta wings of large sweep angles. Alternately, with some blowing or suction, the bursting of the trapped vortices could be postponed to a much higher angle of attack. An experimental study in this direction is being pursued.

Although the present results suggest that the leading-edge fences along with the Gurney flap may well be useful for approach and landing phases of flight at low angles of attack, further study is required for similar takeoff applications. One possible solution could be using leading-edge vortex flaps at a modest upward deflection angle, for example, 30 deg. In this case, the upward leading vortex flap along with the Gurney flap could still produce significant lift increase at low angles of attack, but with a drag favorably lower than the 90-deg fence case. As a result, the combined configuration could be considered for takeoff at low angles of attack.

Acknowledgments

This research was supported by the NASA Ames Research Center Grant NCC 2-730. The authors gratefully acknowledge Vernon Rossow and James Ross for their support and fruitful discussions. The authors also would like to thank Gayle Downs and Eltahry Elghandour for their help with the figures.

References

[1]Rossow, V. J., "Lift Enhancement by an Externally Trapped Vortex," *Journal of Aircraft*, Vol. 15, No. 9, 1978, pp. 618–625.

[2]Rossow, V. J., "Two-Fence Concept for Efficient Trapping of Vortices on Airfoils," *Journal of Aircraft*, Vol. 29, No. 5, 1992, pp. 847–855.

[3]Riddle, T. W., Wadcock, A., Tso, J., and Cummings, R. M., "An Experimental Analysis of Vortex Trapping Techniques," *Journal of Fluids Engineering*, Vol. 121, No. 3, 1999, pp. 555–559.

[4]Buchholz, M. D., Hendrickson, H. C., and Westra, B. W., "Two-Fence Vortex Trapping on a Low Angle-of-Attack Wing," Senior Project Rept., Aerospace Engineering Dept., California Polytechnic State Univ., San Luis Obispo, CA, 1991.

[5]Riddle, T. W., Rogers, S. E., Ross, J. C., and Cummings, R. M., "A Numerical Analysis of Three-Dimensional Vortex Trapping," *Aircraft Design*, Vol. 1, No. 1, 1998, pp. 61–73.

[6]Marchman, J. F., "Aerodynamics of Inverted Leading-Edge Flaps on Delta Wings," *Journal of Aircraft*, Vol. 18, No. 12, 1981, pp. 1051–1056.

[7]Buchholz, M. D., and Tso, J., "Vortex Trapping on a 60-Degree Delta Wing," AIAA Paper 92-2693, June 1992.

[8]Buchholz, M. D., and Tso, J., "Lift Augmentation on a Delta Wing via Leading Edge Fences and the Gurney Flap," AIAA Paper 93-3513, Aug. 1993.

[9]Traub, L. W., and Galls, S. F., "Effects of Leading- and Trailing-Edge Gurney Flaps on a Delta Wing," *Journal of Aircraft*, Vol. 36, No. 4, 1999, pp. 651–658.

[10]Deng, Q., and Gursul, I., "Effect of Leading-Edge Flaps on Vortices and Vortex Breakdown," *Journal of Aircraft*, Vol. 33, No. 6, 1996, pp. 1079–1086.

[11]Giguere, P., Lemay, J., and Dumas, G., "Gurney Effects and Scaling for Low-Speed Airfoils," AIAA Paper 95-1881, June 1995.

[12]Myose, R., Papadakis, M., and Heron, I., "Gurney Flap Experiment on Airfoils, Wings, and Reflection Plane Model," *Journal of Aircraft*, Vol. 35, No. 2, 1998, pp. 206–211.

[13]Liebeck, R. H., "Design of Subsonic Airfoils for High Lift," *Journal of Aircraft*, Vol. 15, No. 9, 1978, pp. 547–561.

[14]Neuhart, D. H., and Pendergraft, O. C., Jr., "A Water Tunnel Study of Gurney Flaps," NASA TM 4071, 1988.

[15]Jang, C. S., Ross, J. C., and Cummings, R. M., "Numerical Investigation of an Airfoil with a Gurney Flap," *Aircraft Design*, Vol. 1, No. 1, 1998, pp. 75–88.

[16]Katz, J., and Largman, R., "Effect of 90-Degree Flap on the Aerodynamics of a Two-Element Airfoil," *Journal of Fluids Engineering*, Vol. 111, No. 1, 1989, pp. 93, 94.

[17]Storms, B. L., and Jang, C. S., "Lift Enhancement of an Airfoil Using a Gurney Flap and Vortex Generators," *Journal of Aircraft*, Vol. 31, No. 3, 1994, pp. 542–547.

[18]Hummel, D., and Srinivasan, P. S., "Vortex Breakdown Effects on the Low-Speed Aerodynamic Characteristics of Slender Delta Wings in Symmetrical Flow," *Journal of the Royal Aeronautical Society*, Vol. 71, No. 676, 1967, pp. 319–322.

[19]Wentz, W. H., Jr., and Kohlman, D. L., "Vortex Breakdown on Slender Sharp-Edged Wings," *Journal of Aircraft*, Vol. 8, No. 3, 1971, pp. 156–161.

[20]Lambourne, N. C., and Bryer, D. W., "The Bursting of Leading-Edge Vortices—Some Observations and Discussion of the Phenomenon," Aeronautical Research Council, Repts. and Memorandums 3282, London, 1961.

[21]Sarpkaya, T., "Vortex Breakdown in Swirling Conical Flows," *AIAA Journal*, Vol. 9, No. 9, 1971, pp. 1792–1799.

[22]Sarpkaya, T., "Effect of the Adverse Pressure Gradient on Vortex Breakdown," *AIAA Journal*, Vol. 12, No. 5, 1974, pp. 602–607.